JOURNAL OF SOLID STATE CHEMISTRY **130,** 234–249 (1997)
ARTICLE NO. SC967210

New Layered Materials in the K–In–Ge–As System: $K_8In_8Ge_5As_{17}$ and $K_5In_5Ge_5As_{14}$

Julie L. Shreeve-Keyer and Robert C. Haushalter[1]

NEC Research Institute, 4 Independence Way, Princeton, New Jersey 08540

Young-Sook Lee, Sichu Li, and Charles J. O'Connor

Department of Chemistry, University of New Orleans, New Orleans, Louisiana 70148

and

Dong-Kyun Seo and Myung-Hwan Whangbo

Department of Chemistry, North Carolina State University, Raleigh, North Carolina 27695

Received July 22, 1996; in revised form October 3, 1996; accepted October 24, 1996

Exploratory synthesis in the K–In–Ge–As system has yielded the unusual layered compounds $K_8In_8Ge_5As_{17}$ (1) and $K_5In_5Ge_5As_{14}$ (2), both of which contain In–Ge–As layers with interleaved potassium ions, Ge–Ge bonds, $InAs_4$ tetrahedra, As–As bonds, and rows of Ge_2As_6 dimers. Compound 1 has As_3 groups, while compound 2 has infinite As ribbons on both faces of each layer. Unlike compound 1, compound 2 has substitutional defects where indium partially occupies each of the three independent germanium sites in the ratio of 1:5 for In:Ge. This partial occupancy makes 2 an electron-precise compound. The Ge(In)–Ge(In) bond of 2 is longer than the Ge–Ge bond of 1, and this bond lengthening effect was confirmed by performing DFT-MO calculations on the model compounds $H_3Ge–GeH_3$ and $H_3Ge–InH_3^-$. Possible implications of electron imprecise formulas determined by X-ray crystal structure determinations are discussed. Compound 1: space group $P2_1/c$ with $a = 18.394\ (8)$ Å, $b = 19.087\ (7)$ Å, $c = 25.360\ (3)$ Å, $\beta = 105.71\ (2)°$, $V = 8571\ (4)$ Å^3, and $D_{calcd} = 4.45$ g/cm^3 for $Z = 4$. Refinement on 4455 reflections yielded $R(R_w) = 6.8\%(7.8\%)$. Compound 2: space group $C2/m$ with $a = 40.00\ (1)$ Å, $b = 3.925\ (2)$ Å, $c = 10.299\ (3)$, $\beta = 99.97\ (2)°$, $V = 1592\ (1)$ Å^3, and $D_{calcd} = 4.55$ g/cm^3 for $Z = 8$. Refinement on 1206 reflections yielded $R(R_w) = 5.6\%\ (5.7\%)$. © 1997 Academic Press

INTRODUCTION

The Zintl phase materials comprise an interesting class of solids that can, in a certain sense, be considered as possessing properties intermediate between those of ionic salts and metals or intermetallic phases. In the synthesis of these compounds, reaction between an alkali or alkaline earth metal and a heavier post-transition element results in electron transfer from the more electropositive elements to the electronegative elements. The resulting isolated anions and polyanions often possess extensive element–element bonding to complete the octet of electrons in their valence orbitals. Zintl alloys are frequently prepared by heating a direct combination of the elements or the elements with simple binary phases. For example, KSn may be prepared by mixing molten potassium and molten tin to give KSn (1a,b). Similar synthetic techniques can be used to produce KPb (1c), KSb (1d), KTl (1b), K_5In_8 (1e), K_5Ga_8 (1f), and others, which may be isolated and identified by powder diffraction.

Recently there has been much interest in Zintl phase materials with a number of structurally interesting ternary materials being prepared. Investigations by von Schnering (2), Schäfer (3), Corbett (4), and others (5) have shown that Zintl phases possess a huge number of novel structure types, bonding schemes, and unusual physical properties. While most of these studies have focused on the preparative and structural aspects of the materials, there are a few examples of the low temperature preparation of metastable materials, such as thin films (6) and amorphous metallic spin glasses (7). Synthesis of ternary I–III–V Zintl phase materials as a preliminary step in the investigation of new routes to the preparation of III–V type semiconductors has also been of interest (5g).

While there are several examples of ternary Zintl phase materials (2–5), there are apparently no examples containing four elements from different groups of the periodic

---

[1] Present address: Symyx Technologies, 420 Oakmead Parkway, Sunnyvale, CA 94086.

0022-4596/97 $25.00
Copyright © 1997 by Academic Press
All rights of reproduction in any form reserved.

table present in a stoichiometric, ordered fashion. We have undertaken an exploratory synthetic investigation of Group 1-13-14-15 quaternary Zintl phases to determine if it is possible to incorporate such a large number of elements into a crystalline material and how the structure and composition would influence the physical properties. We report here the synthesis and single crystal X-ray structures of $K_8In_8Ge_5As_{17}$ (**1**) and $K_5In_5Ge_5As_{14}$ (**2**) both of which contain structurally complex In–Ge–As layers interleaved with K^+ ions.

EXPERIMENTAL PROCEDURES

All compounds described here are extremely air- and moisture-sensitive. All manipulations were performed under a high-purity inert gas atmosphere. Caution: *Arsenic compounds are toxic*. The preparations in this paper involve the use of arsenic at high temperatures; therefore, appropriate precautions should be taken. These precautions include working on small scales, heating the sealed tubes in a quartz lined furnace which is contained inside a fume hood, as well as good laboratory hygiene. The elements K (99.95%), In (99.999%), Ge (>99.999%), As (99.999%), and Ba (99.7%) were purchased from Cerac. The solid of nominal composition K_3As_7 was made by fusing a stoichiometric amount of the elements in a quartz tube under argon. Energy dispersive X-ray spectroscopy (EDS) was performed using a Princeton Gamma Technology EDS detector mounted on a Hitachi S-2700 SEM. Powder X-ray data was obtained from a Scintag XDS 2000.

Preparation of $K_8In_8Ge_5As_{17}$ (**1**). The elements K (0.117 g, 2.99 mmol), In (0.206 g, 1.79 mmol), Ge (0.087 g, 1.20 mmol), and As (0.359 g, 4.79 mmol) were combined in a mole ratio of 5 : 3 : 2 : 8 and then sealed into an evacuated quartz ampoule. This mixture was heated to 871°C over 8 h (106°/h), where the temperature was held for another 6 h. X-ray quality crystals were obtained by slowly cooling the tube to 482°C over 20 h (19.5°/h) and then to ambient temperature over 15 h. This method gave a heterogeneous mixture, which contained X-ray quality crystals of **1**, as well as GeAs and InAs, which were identified by powder X-ray diffraction measurements. Several attempts to synthesize **1** from stoichiometric mixtures of the elements were made, which did not result in single phase products.

Preparation of $K_5In_5Ge_5As_{14}$ (**2**). The solids K_3As_7 (0.500 g, 0.779 mmol), Ba (0.024 g, 0.175 mmol), In (0.314 g, 2.73 mmol), and Ge (0.124 g, 1.71 mmol) were combined in a mole ratio of 5 : 1 : 16 : 10 and then sealed in an evacuated quartz ampoule. This mixture was heated to 750°C over 12 h (60.5°/h). The temperature was held at 750°C for 6 h, then slowly cooled to 550°C at 4°/h, followed by cooling to ambient temperature over 6 h. This method gave a heterogeneous mixture, which contained X-ray quality crystals of **2**, which appear as silver needles throughout the reaction mixture, as well as GeAs, InAs, Ge, and As, according to powder X-ray diffraction measurements. EDS analysis of **2** showed only K, In, Ge, and As, and no Ba. We were unable to prepare **2** as a single phase product, or without the addition of barium to the reaction mixture.

X-ray diffraction analysis of $K_8In_8Ge_5As_{17}$ (**1**). A black cubic-shaped crystal of approximate dimensions 0.10 × 0.10 × 0.10 mm was sealed into a glass capillary under an inert atmosphere of helium. Crystals of **1** are extremely sensitive not only to air or moisture, but also to any type of grease or oil, and rapidly exfoliate in the presence of either. Therefore compound **1** must be mounted without the use of any grease or hydrocarbons. The X-ray intensity data were collected on a Rigaku AFC7R automatic four-circle diffractometer equipped with Mo$K\alpha$ radiation and an RU300 18 kW rotating anode generator. Cell constants and an orientation matrix for data collection were obtained from the setting angles of 25 carefully centered reflections in the range $20.07° \leq 2\theta \leq 27.93°$ and corresponded to a primitive monoclinic cell with the unit cell dimensions given in Table 1. The systematic absences of $h0l$: $l \neq 2n$ and $0k0$: $k \neq 2n$ uniquely determined the space group to be $P2_1/c$ (No. 14).

TABLE 1
Experimental Crystallographic Details for $K_8In_8Ge_5As_{17}$ (1) and $K_5In_5Ge_5As_{14}$ (2)

	1	2
Formula	$K_{16}In_{16}Ge_{10}As_{34}$	$K_{1.25}In_{1.25}Ge_{1.25}As_{3.5}$
Formula weight	2867.96	545.36
Temperature (°C)	20	20
Crystal color, habit	black, cube	silver, needle
Crystal dimensions (mm)	ca. 0.10 × 0.10 × 0.10	ca. 0.20 × 0.05 × 0.03
Crystal system	monoclinic	monoclinic
Space group	$P2_1/c$ (#14)	$C2/m$ (#12)
a (Å)	18.396 (7)	40.00 (1)
b (Å)	19.087 (7)	3.925 (2)
c (Å)	25.359 (4)	10.299 (3)
β (°)	105.71 (2)	99.97 (2)
Volume (Å^3)	8571 (4)	1592 (1)
Z	4	8
D_{calc} (g/cm^3)	4.444	4.549
F_{000}	10120.00	1890.00
μ(Mo$K\alpha$) (cm^{-1})	214.74	232.83
Diffractometer	Rigaku AFC7R	Rigaku AFC7R
Scan type	ω-2θ	ω-2θ
Scan rate (deg/min)	8.0	16.0
$2\theta_{max}$	50.1°	60.1°
Reflections measured	Total: 8543 Unique: 8205	Total: 2514 Unique: 2418
Observations ($I > 3.00\sigma(I)$)	4455	1206
No. of variables	518	104
R, R_w	6.5%, 7.5%	5.6%, 5.7%
Goodness of fit	3.78	2.87
Max. peak in final diff. map	2.67 e/Å^3	1.97 e/Å^3
Min. peak in final diff. map	− 2.05 e/Å^3	− 2.99 e/Å^3

The data collection consisted of scans of $(1.31 + 0.35\tan\theta)^\circ$ in the range $5^\circ \leq 2\theta \leq 50.1^\circ$ which were made using the ω-2θ scan technique at a speed of 8.0°/min (in omega). The weak reflections $[I < 20\sigma(I)]$ were rescanned a maximum of three times, and the counts were accumulated to ensure good counting statistics. Stationary background counts were recorded on each side of the reflection. The ratio of peak counting time to background counting time was 2 : 1. The diameter of the incident beam collimator was 0.5 mm and the crystal to detector distance was 400 mm. The intensities of 3 standard reflections were measured after every 150 reflections and, over the course of data collection, decreased in intensity by 1.7%. A linear correction factor was applied to the data to account for this phenomenon. An empirical absorption correction using the program DIFABS (8) was also applied in the final stages of refinement, and resulted in transmission factors ranging from 0.87 to 1.15. The data were also corrected for Lorentz and polarization effects.

The structure was solved by direct methods (9a) and refined on F by full-matrix least-squares using the *teXsan* crystallographic software package of Molecular Structure Corporation (10). The potassium, indium, and germanium atoms were refined anisotropically, while the arsenic atoms were refined isotropically. The final least-squares refinement was based on 4455 observed reflections $[I > 3.0\sigma(I)]$ and 518 variable parameters, and converged with $R(R_w) = 0.065(0.075)$, with GOF = 3.78 and $\rho(\max) = 2.67\ \mathrm{e\AA^{-3}}$, $\rho(\min) = -2.05\ \mathrm{e\AA^{-3}}$. Further details of the X-ray structural analysis of compound **1** are given in Table 1. The final positional and equivalent isotropic displacement parameters are given in Table 2.

TABLE 2
Atomic Coordinates and B_{iso} for $K_8In_8Ge_5As_{17}$ (1)

Atom	x	y	z	B_{iso}
In(1)	0.1688(3)	−0.2762(2)	0.8463(2)	1.8(2)
In(2)	0.1024(3)	0.0429(2)	0.8690(2)	1.8(2)
In(3)	0.9570(3)	0.0420(2)	0.7201(2)	1.5(2)
In(4)	0.0031(3)	−0.2752(2)	0.6829(2)	2.0(2)
In(5)	0.8527(3)	−0.2677(2)	0.5773(2)	1.8(2)
In(6)	0.8066(3)	0.0357(2)	0.5711(2)	1.6(2)
In(7)	0.6587(3)	0.0147(2)	0.4185(2)	1.8(2)
In(8)	0.5029(3)	0.0176(2)	0.3143(2)	1.6(2)
In(9)	0.2577(3)	−0.2742(2)	−0.0191(2)	1.6(2)
In(10)	0.2531(3)	0.0176(2)	0.0197(2)	1.9(2)
In(11)	0.2894(3)	0.2116(2)	0.0743(2)	1.8(2)
In(12)	0.3360(3)	0.0199(2)	0.1523(2)	1.8(2)
In(13)	0.5534(3)	−0.3008(2)	0.2804(2)	1.7(2)
In(14)	0.4108(3)	−0.2985(2)	0.1319(2)	1.8(2)
In(15)	0.0943(3)	−0.1019(2)	0.7660(2)	1.7(2)
In(16)	0.4226(3)	−0.1542(2)	0.2318(2)	2.4(2)
As(1)	0.0218(4)	−0.0667(3)	0.8902(3)	1.8(1)
As(2)	0.1080(4)	−0.2574(3)	0.9295(2)	1.2(1)
As(3)	0.2497(4)	0.0255(3)	0.9166(3)	1.8(1)
As(4)	0.2797(4)	−0.3627(3)	0.9087(3)	1.6(1)
As(5)	0.2256(4)	−0.1541(3)	0.8203(3)	1.6(1)
As(6)	0.1016(4)	0.0353(3)	0.7657(3)	1.9(1)
As(7)	0.8842(4)	−0.0622(3)	0.7537(3)	1.5(1)
As(8)	0.8918(4)	0.1558(3)	0.7444(3)	1.4(1)
As(9)	0.8602(4)	−0.2514(3)	0.6849(3)	1.4(1)
As(10)	0.9630(4)	−0.3556(3)	0.5900(3)	1.4(1)
As(11)	0.0684(4)	−0.1545(3)	0.6655(3)	1.5(1)
As(12)	0.9540(4)	0.0309(3)	0.6157(3)	1.6(1)
As(13)	0.7073(4)	−0.2694(3)	0.5276(3)	1.5(1)
As(14)	0.9195(4)	−0.1605(3)	0.5325(3)	1.3(1)
As(15)	0.7782(4)	−0.1760(3)	0.3865(3)	1.7(1)
As(16)	0.8028(4)	0.0184(3)	0.4666(3)	1.5(1)
As(17)	0.5624(4)	−0.2871(3)	0.3865(3)	1.6(1)
As(18)	0.5951(4)	−0.0932(3)	0.4623(3)	1.3(1)
As(19)	0.5375(4)	0.0929(3)	0.4086(3)	2.0(1)
As(20)	0.4464(4)	−0.1042(3)	0.3309(3)	1.6(1)
As(21)	0.6476(4)	−0.0043(3)	0.3108(3)	1.9(1)
As(22)	0.4099(4)	−0.2906(3)	0.2338(3)	1.6(1)
As(23)	0.6293(4)	−0.2003(3)	0.2454(3)	1.6(1)
As(24)	0.6091(4)	−0.4169(3)	0.2531(3)	1.7(1)
As(25)	0.4918(4)	−0.1922(3)	0.1062(3)	1.7(1)
As(26)	0.3494(4)	−0.1657(3)	−0.0352(3)	1.5(1)
As(27)	0.0168(4)	0.1403(3)	0.1919(3)	1.4(1)
As(28)	0.2672(4)	−0.2834(3)	0.0848(3)	1.5(1)
As(29)	0.4029(4)	0.0006(3)	0.0724(3)	1.9(1)
As(30)	0.1656(4)	−0.0918(3)	0.0338(3)	1.2(1)
As(31)	0.2187(4)	0.0979(3)	0.0932(3)	1.7(1)
As(32)	0.2910(4)	−0.1044(3)	0.1785(3)	1.7(1)
As(33)	0.2590(4)	0.0769(3)	0.3934(3)	1.4(1)
As(34)	0.4673(4)	0.1190(3)	0.8108(3)	1.7(1)
Ge(1)	0.1319(4)	−0.1342(3)	0.9397(3)	1.7(3)
Ge(2)	0.2411(4)	−0.1010(3)	0.9092(3)	1.9(3)
Ge(3)	0.8579(4)	−0.1276(3)	0.6672(3)	2.0(3)
Ge(4)	0.9510(4)	−0.0964(3)	0.6192(3)	1.7(3)
Ge(5)	0.7104(4)	−0.1438(3)	0.5196(3)	1.5(3)
Ge(6)	0.8051(4)	−0.1092(3)	0.4736(3)	1.5(3)
Ge(7)	0.5651(4)	−0.1599(3)	0.3774(3)	1.8(3)
Ge(8)	0.6582(4)	−0.1286(3)	0.3286(3)	1.7(3)
Ge(9)	0.2742(4)	−0.1566(3)	0.0893(3)	1.6(3)
Ge(10)	0.3838(4)	−0.1219(3)	0.0587(3)	1.9(3)
K(1)	0.0000	0.0000	0.0000	9(2)
K(2)	0.882(1)	0.0485(7)	0.8533(6)	2.9(8)
K(3)	0.431(1)	0.099(1)	0.977(1)	7(1)
K(4)	0.732(1)	0.0409(7)	0.7068(7)	2.8(7)
K(5)	0.519(1)	0.2078(8)	0.5066(8)	5(1)
K(6)	0.4173(9)	−0.0229(7)	0.4434(6)	2.6(7)
K(7)	0.373(1)	0.1863(7)	0.3584(7)	3.6(8)
K(8)	0.227(1)	0.1794(7)	0.2104(7)	3.2(8)
K(9)	0.066(1)	0.1948(8)	0.0509(8)	4(1)
K(10)	0.3784(8)	−0.2474(7)	0.8547(6)	2.4(7)
K(11)	0.042(1)	0.1850(7)	0.6802(6)	3.1(7)
K(12)	0.0000	0.0000	0.5000	4(1)
K(13)	0.837(1)	0.0040(8)	0.3449(6)	3.3(8)
K(14)	0.7726(9)	0.2387(7)	0.2942(6)	2.2(7)
K(15)	0.267(1)	0.111(1)	0.8123(8)	5(1)
K(16)	0.442(1)	−0.4426(8)	0.3185(8)	5(1)
K(17)	0.913(1)	0.235(1)	0.4452(9)	7(1)

Note. $B_{\mathrm{eq}} = \frac{8}{3}\pi^2(U_{11}(aa^*)^2 + U_{22}(bb^*)^2 + U_{33}(cc^*)^2 + 2U_{12}aa^*bb^*\cos\gamma + 2U_{13}aa^*cc^*\cos\beta + 2U_{23}bb^*cc^*\cos\alpha)$.

X-ray diffraction analysis of $K_5In_5Ge_5As_{14}$ (**2**). A silver needle-shaped crystal of approximate dimensions 0.05 × 0.03 × 0.20 mm was sealed into a glass capillary under an inert atmosphere of helium. X-ray intensity data were collected on a Rigaku AFC7R automatic four-circle diffractometer equipped with Mo$K\alpha$ radiation and an RU300 18 kW rotating anode generator. Cell constants and an orientation matrix for data collection were obtained from the setting angles of 25 carefully centered reflections in the range $20.48° \leq 2\theta \leq 24.94°$ and corresponded to a C-centered monoclinic cell with the unit cell dimensions given in Table 1. Based on the systematic absences of hkl: $h + k \neq 2n$, a statistical analysis of the intensity distribution, and the successful solution and refinement of the structure, the space group was determined to be $C2/m$ (No. 12).

The data collection consisted of scans of $(1.47 + 0.35 \tan \theta)°$ in the range $5.0° \leq 2\theta \leq 60.1°$ which were made using the ω-2θ scan technique at a speed of 16.0°/min (in omega). The weak reflections $[I < 20\sigma(I)]$ were rescanned a maximum of four times, and the counts were accumulated to ensure good counting statistics. Stationary background counts were recorded on each side of the reflection. The ratio of peak counting time to background counting time was 2 : 1. The diameter of the incident beam collimator was 0.5 mm and the crystal to detector distance was 400 mm. The intensities of 3 standard reflections were measured after every 150 reflections and, over the course of data collection, decreased in intensity by 1.2%. A linear correction factor was applied to the data to account for this phenomenon. An empirical absorption correction using the program DIFABS (8) was also applied in the final stages of refinement and resulted in transmission factors ranging from 0.80 to 1.00. The data were also corrected for Lorentz and polarization effects.

TABLE 3
Atomic Coordinates and B_{iso} for $K_5In_5Ge_5As_{14}$ (2)

Atom	x	y	z	occ	B_{iso}
In(1)	0.22675(9)	−0.5000	0.1681(3)	0.083[a]	1.32(5)
In(2)	0.20156(8)	−0.5000	−0.0791(3)	0.083[a]	1.16(5)
In(3)	0.02021(9)	0.0000	0.4188(3)	0.083[a]	1.74(6)
In(4)	0.14839(5)	0.0000	0.1295(2)	0.500	1.62(4)
In(5)	0.07255(6)	−0.5000	0.2333(2)	0.500	2.71(5)
As(1)	0.26208(7)	0.0000	0.2507(3)	0.500	2.01(6)
As(2)	0.16237(8)	0.0000	−0.1136(3)	0.500	2.04(6)
As(3)	0.17608(7)	−0.5000	0.2716(2)	0.500	1.67(5)
As(4)	0.08230(8)	0.0000	0.0909(3)	0.500	2.40(6)
As(5)	0.10743(8)	−0.5000	0.4659(3)	0.500	3.29(8)
As(6)	0.07831(8)	0.0000	0.5540(3)	0.500	2.68(7)
As(7)	0.01020(8)	−0.5000	0.2701(3)	0.500	2.48(6)
Ge(1)	0.22675(9)	−0.5000	0.1681(3)	0.417[b]	1.32(6)
Ge(2)	0.20156(8)	−0.5000	−0.0791(3)	0.417[b]	1.16(6)
Ge(3)	0.02021(9)	0.0000	0.4188(3)	0.417[b]	1.74(6)
K(1)	0.1807(2)	0.0000	0.5454(7)	0.500	4.2(2)
K(2)	0.0000	0.0000	0.0000	0.250	5.6(3)
K(3)	−0.0877(2)	−0.5000	0.1755(6)	0.500	3.2(2)

Note. $B_{eq} = \frac{8}{3}\pi^2(U_{11}(aa^*)^2 + U_{22}(bb^*)^2 + U_{33}(cc^*)^2 + 2U_{12}aa^*bb^*\cos\gamma + 2U_{13}aa^*cc^*\cos\beta + 2U_{23}bb^*cc^*\cos\alpha)$.

[a] 1/6 In occupancy at Wyckoff *i* site.

[b] 5/6 Ge occupancy at Wyckoff *i* site.

The structure was solved by direct methods (9b) and refined on F by full-matrix least-squares using the *teXsan* crystallographic software package of Molecular Structure Corporation (10). All atoms were refined anisotropically. The final least-squares refinement was based on 1206 observed reflections $[I > 3.0\sigma(I)]$ and 104 variable parameters and converged with $R(R_w) = 0.056(0.057)$, with GOF = 2.87 and $\rho(\max) = 1.97\,e\text{Å}^{-3}$, $\rho(\min) = -2.99\,e\text{Å}^{-3}$. Further details of the X-ray structural analysis of compound **2** are given in Table 1. The final positional and equivalent isotropic displacement parameters are given in Table 3.

Supplementary material available. Tables giving crystal data and details of the structure determination, atomic coordinates, anisotropic thermal parameters, and bond lengths and angles are available.[1]

RESULTS AND DISCUSSION

Crystal Structures

Thermal treatment of mixtures of K, In, Ge, and As or K_3As_7, In, Ge, and Ba in evacuated, sealed quartz ampoules yielded X-ray quality single crystals of the unusual compounds $K_8In_8Ge_5As_{17}$ (**1**) and $K_5In_5Ge_5As_{14}$ (**2**), respectively. Both compounds **1** and **2** were isolated as crystals from a heterogeneous mixture of products. Several attempts to synthesize **1** and **2** from stoichiometric mixtures of the elements and K_3As_7 were made. These attempts did not lead to single phase products, but continued to produce heterogeneous mixtures from which **1** and **2** could be isolated. Attempts to synthesize **2** without the addition of barium to the reaction mixture was attempted, but this did not lead to the formation of **2**. The necessity of the presence of barium on the formation of **2** is not clear at this time.

The structures of **1** and **2** have several similar features. First, both structures have potassium ions which lie between layers comprised of In, Ge, and As. However, compound **1**

---

[1] See NAPS document No. 00000 for 27 pages of supplementary material. This is __ is not __ a multi-article document. Order from NAPS c/o Microfiche Publications, P.O. Box 3513, Grand Central Station, New York, NY 10163-3513. Remit in advance in U.S. funds only $7.75 for photocopies or $5.00 for microfiche. There is a $15.00 invoicing charge on all orders filled before payment. Outside U.S. and Canada add postage of $4.50 for the first 20 pages and $1.00 for each 10 pages of material thereafter, or $1.75 for the first microfiche and 50 ¢ for each microfiche thereafter.

also has potassium ions situated within dimples in the layer. Second, both structures contain rows of Ge_2As_6 dimers with Ge–Ge bonds, as well as $InAs_4$ tetrahedra, and As–As bonds. Assignment of the Ge and As atoms was based on connectivity (Ge is four-coordinate tetrahedral and As three coordinate), as these two atoms are difficult to distinguish by X-ray diffraction.

The structure of compound **1** contains layers with the composition $[In_8Ge_5As_{14}(As_3)]^{8-}$, which run parallel to the $(1\,0\,\bar{1})$ plane and are separated by ca. 11 Å (Fig. 1). These

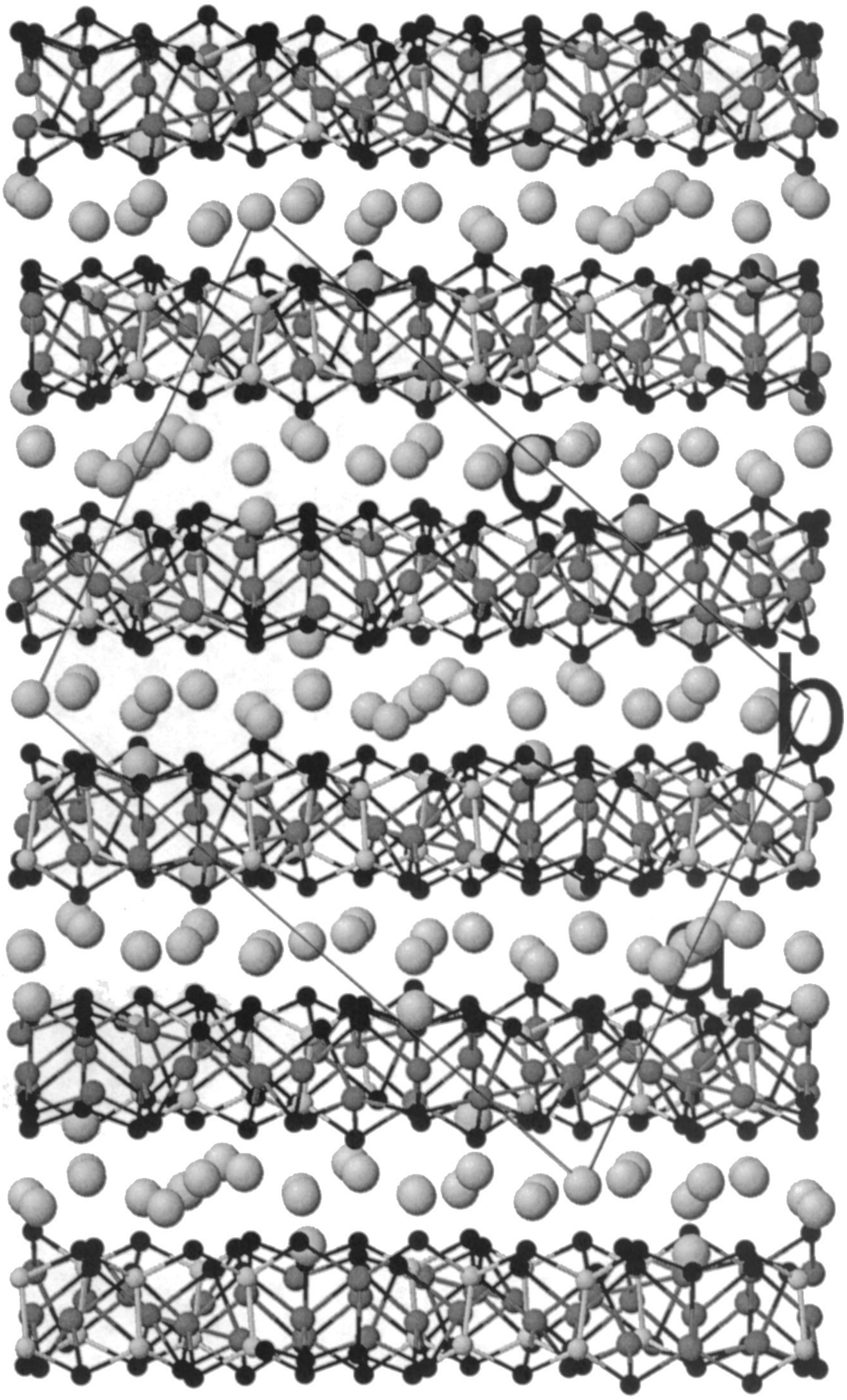

FIG. 1. View of $K_8In_8Ge_5As_{17}$ (**1**) showing the layers comprised of indium, germanium, and arsenic atoms, separated by potassium cations. The arsenic atoms are shown in black, the indium atoms in dark gray, and the germanium and potassium atoms in light gray.

structurally complex In–Ge–As layers are separated by potassium cations. A small section of the layer can be seen more clearly in Fig. 2, which shows a ball and stick representation of a section of one layer in compound **1**, as well as the numbering scheme used for the indium, germanium, and arsenic atoms. The row of Ge_2As_6 dimers contains a periodic substitution of two $InAs_4$ tetrahedra which are centered about In(15) and In(16). The $InAs_4$ tetrahedra formed from In(1) and In(9), In(4) and In(5), In(7) and In(8), and those from In(10) and In(12) share a common edge. The other $InAs_4$ tetrahedra above and below the row of Ge dimers are each linked through only one arsenic atom to each neighboring germanium or indium atom.

Figure 3a shows a polyhedral representation of a single layer in compound **1**. Each layer contains a row of corner-sharing Ge_2As_6 dimers, in which the Ge–Ge bond is nearly perpendicular to the plane of the layer. Some Ge_2As_6 moieties along a row are periodically replaced by $InAs_4$ tetrahedra, such that along a given row there are two Ge_2As_6 dimers, one $InAs_4$ tetrahedron, three Ge_2As_6 dimers, and then another $InAs_4$ tetrahedron. In the locations where a single $InAs_4$ unit replaces a Ge_2As_6 fragment, the As atoms link via As–As bonds to satisfy their coordination change resulting from the "missing" metal atom to form an As_3 unit with two As–As bonds. The end As atoms in the As_3 trimer are from a corner-sharing interaction between a Ge_2As_6 dimer and an $InAs_4$ tetrahedra. The center As atom in the As_3 unit is from a vertex of a $InAs_4$ tetrahedron and is not linked to any other polyhedra.

Selected bond distances for compound **1** are given in Table 4. The average Ge–Ge distances in the Ge_2As_6 dimers in **1** is 2.43 (1) Å and the average Ge–As bond length is 2.43 (2) Å with a 2.377 (8) to 2.481 (9) Å range of distances. The As_3 trimers contain As–As bonds in the range from 2.451 (9) to 2.495 (9) Å, and As–As–As angles of 97.4 (3)° and 98.1 (3)°.

The previously described rows are linked by two irregular rows of $InAs_4$ tetrahedra, such that the $InAs_4$ tetrahedra are corner-shared with the Ge_2As_6 dimers. Each $InAs_4$ spans a Ge_2As_6 dimer, as well serving to connect the dimer to the next Ge_2As_6 dimer. At the point where the Ge dimers are substituted by an $InAs_4$ tetrahedron, two $InAs_4$ units from the adjacent chain, which are corner-shared with the substituted $InAs_4$ tetrahedron, each form an edge-sharing arrangement with neighboring $InAs_4$ units within the row. The two edge-shared polyhedra meet with another $InAs_4$ tetrahedra from the next adjacent row at one shared As atom. This pattern creates a puckering, or pocket, in the layer where the three $InAs_4$ tetrahedra meet.

The resulting dimples display free dimensions of approximately 3.7 Å wide ($= d$ (As to As) $- 2r_{As}$) and 2.4 Å deep ($= d$ (plane defined by five As centroids to the As centroid in the bottom of the dimple) $- r_{As}$) and each contain one potassium whose center is located approximately 1 Å above the plane described by the centers of the five arsenic atoms around the perimeter of the dimple. There are two crystallographically independent dimples which contain potassium atoms K(11) and K(16), respectively, in the asymmetric unit. The space-filling model shown in Fig. 4 is a cross-section of the layer showing a dimple with the potassium ion shown in black, situated within the depression. Figure 5 shows the coordination environment of the potassium atoms within the cavities of compound **1**. The five K–As distances to the perimeter As atoms range from 3.39 (1) to 3.62 (2) Å. These K atoms in the cavities are much closer to one layer than the other, with the closest K–As distance to the next layer being 4.11 (2) Å. The other

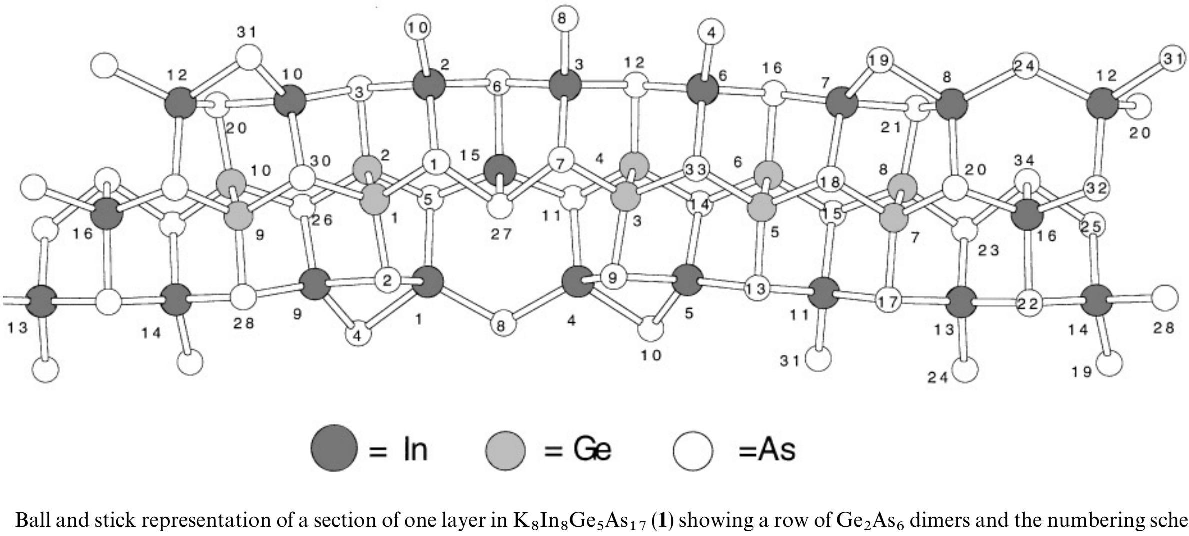

FIG. 2. Ball and stick representation of a section of one layer in $K_8In_8Ge_5As_{17}$ (**1**) showing a row of Ge_2As_6 dimers and the numbering scheme for the indium, germanium, and arsenic atoms.

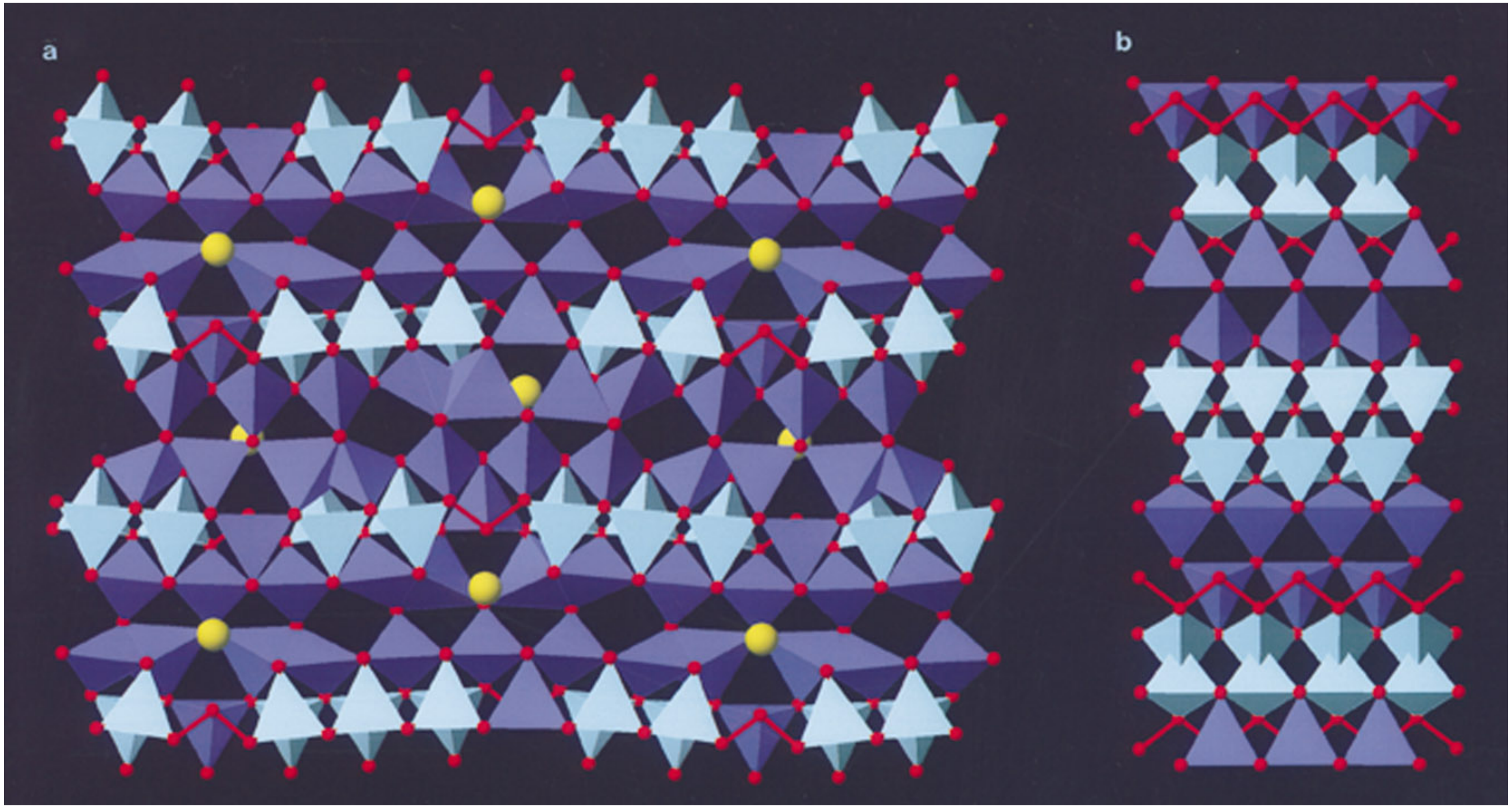

FIG. 3. (a) Polyhedral representation of a single layer in **1**. (b) Polyhedral representation of a single layer in **2**. The Ge_2As_6 are represented by the pale blue polyhedra, and the $InAs_4$ by the indigo polyhedra, As atoms in red, and K atoms in yellow.

TABLE 4
Selected Bond Distances (Å) for $K_8In_8Ge_5As_{17}$ (1)

Atom	Atom	Distance	Atom	Atom	Distance	Atom	Atom	Distance
In(1)	In(9)	3.363(6)	In(6)	As(4)	2.642(8)	In(11)	As(15)	2.794(8)
In(1)	As(2)	2.669(9)	In(6)	As(12)	2.643(8)	In(11)	As(17)	2.636(8)
In(1)	As(4)	2.765(7)	In(6)	As(16)	2.652(9)	In(11)	As(31)	2.641(8)
In(1)	As(5)	2.707(8)	In(6)	As(33)	2.734(8)	In(12)	As(24)	2.630(8)
In(1)	As(8)	2.612(7)	In(7)	In(8)	3.331(6)	In(12)	As(29)	2.66(1)
In(2)	As(1)	2.701(8)	In(7)	As(16)	2.601(8)	In(12)	As(31)	2.714(7)
In(2)	As(3)	2.673(8)	In(7)	As(18)	2.746(8)	In(12)	As(32)	2.656(8)
In(2)	As(6)	2.619(9)	In(7)	As(19)	2.638(8)	In(13)	As(17)	2.664(9)
In(2)	As(10)	2.639(8)	In(7)	As(21)	2.708(9)	In(13)	As(22)	2.591(9)
In(3)	As(6)	2.601(9)	In(8)	As(19)	2.713(8)	In(13)	As(23)	2.662(8)
In(3)	As(7)	2.663(8)	In(8)	As(20)	2.629(8)	In(13)	As(24)	2.611(8)
In(3)	As(8)	2.636(8)	In(8)	As(21)	2.719(9)	In(14)	As(19)	2.605(8)
In(3)	As(12)	2.642(9)	In(8)	As(24)	2.612(7)	In(14)	As(22)	2.594(9)
In(4)	In(5)	3.292(6)	In(9)	As(2)	2.728(8)	In(14)	As(25)	2.699(8)
In(4)	As(8)	2.633(7)	In(9)	As(4)	2.603(8)	In(14)	As(28)	2.603(8)
In(4)	As(9)	2.683(9)	In(9)	As(26)	2.770(8)	In(15)	As(5)	2.632(8)
In(4)	As(10)	2.741(8)	In(9)	As(28)	2.598(9)	In(15)	As(6)	2.622(7)
In(4)	As(11)	2.689(8)	In(10)	In(12)	3.295(6)	In(15)	As(11)	2.660(8)
In(5)	As(9)	2.713(8)	In(10)	As(3)	2.602(9)	In(15)	As(27)	2.65(1)
In(5)	As(10)	2.584(8)	In(10)	As(29)	2.738(8)	In(16)	As(20)	2.612(8)
In(5)	As(13)	2.631(8)	In(10)	As(30)	2.719(8)	In(16)	As(22)	2.617(7)
In(5)	As(14)	2.784(8)	In(10)	As(31)	2.619(9)	In(16)	As(32)	2.610(8)
As(1)	As(27)	2.451(9)	In(11)	As(13)	2.625(9)	In(16)	As(34)	2.63(1)
As(1)	Ge(1)	2.440(9)	As(14)	Ge(6)	2.432(9)	As(25)	As(34)	2.469(9)
As(2)	Ge(1)	2.395(8)	As(15)	Ge(6)	2.481(9)	As(25)	Ge(10)	2.430(9)
As(3)	Ge(2)	2.425(8)	As(15)	Ge(8)	2.469(9)	As(26)	Ge(2)	2.443(9)
As(5)	Ge(2)	2.42(1)	As(16)	Ge(6)	2.440(8)	As(26)	Ge(10)	2.439(9)
As(7)	As(27)	2.468(8)	As(17)	Ge(7)	2.439(9)	As(28)	Ge(9)	2.425(8)
As(7)	Ge(3)	2.455(9)	As(18)	Ge(5)	2.424(9)	As(29)	Ge(10)	2.377(8)
As(9)	Ge(3)	2.404(8)	As(18)	Ge(7)	2.432(9)	As(30)	Ge(1)	2.437(9)
As(11)	Ge(4)	2.429(9)	As(20)	Ge(7)	2.428(9)	As(30)	Ge(9)	2.445(9)
As(12)	Ge(4)	2.432(8)	As(21)	Ge(8)	2.414(8)	As(32)	Ge(9)	2.41(1)
As(13)	Ge(5)	2.407(8)	As(23)	As(34)	2.495(9)	As(33)	Ge(3)	2.476(9)
As(14)	Ge(4)	2.446(9)	As(23)	Ge(8)	2.449(9)	As(33)	Ge(5)	2.478(9)
Ge(1)	Ge(2)	2.42(1)	Ge(5)	Ge(6)	2.44(1)	Ge(7)	Ge(8)	2.44(1)
Ge(3)	Ge(4)	2.43(1)	Ge(9)	Ge(10)	2.44(1)			

K atoms are more equally spaced between the layers, as can be seen in Fig. 1, with typical K–As distances from layer to layer ranging from 3.30 (2) to 3.79 (2) Å, as given for K(9).

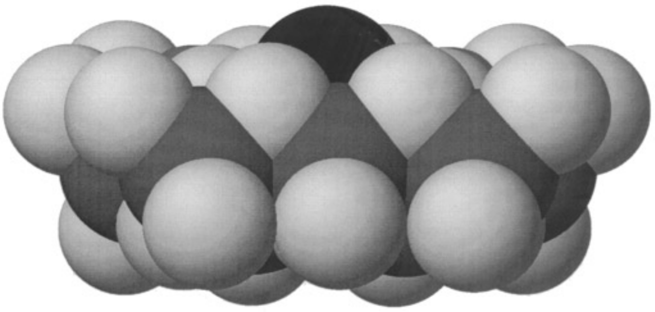

FIG. 4. Space-filling model of a cross-section of one layer in compound **1**, showing the depression in the layer containing the K cation (black), In atoms dark gray, and As atoms light gray.

Potassium arsenic distances for compound **1** are given in Table 5. The potassium atoms other than K(11) and K(16), which are situated in dimples, are more centered between the layers and their coordination environments are shown in Fig. 6. One potassium atom, K(3), is four-coordinate with a see-saw geometry. There are three potassium atoms which are five-coordinate, K(5), K(7), and K(15). Potassium atoms K(5) and K(15) each have a long contact with one potassium atom (3.75 (2) and 3.70 (2) Å, respectively). The geometry of K(5) and K(7) is best described as a severely distorted square pyramid. The atoms K(1), K(6), K(12), and K(13) are six-coordinate with distorted octahedral coordination geometry, with K(1) and K(13) each having one longer contact to an arsenic atom. Other six-coordinate potassium atoms are K(9), K(10), K(14), and K(17) which are coordinated by the arsenic atoms to give distorted trigonal prisms. Potassium atoms K(2), K(4), and K(8), are seven-coordinate, with
]

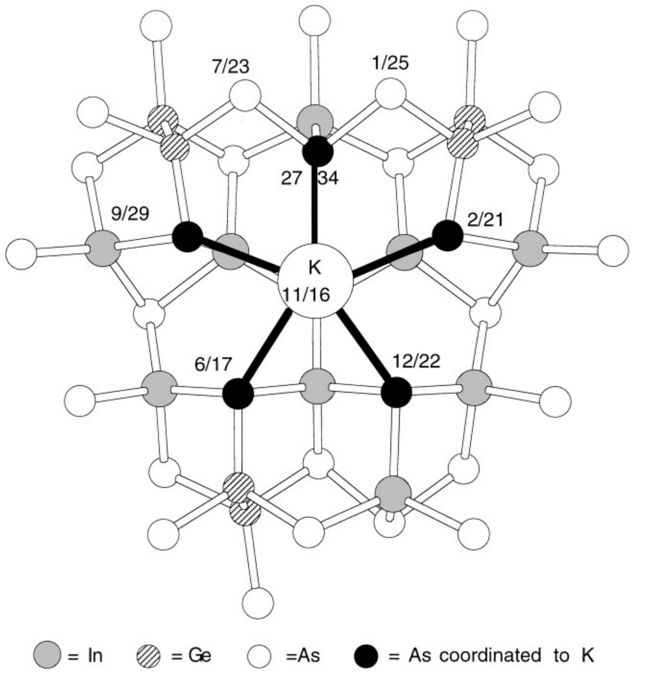

FIG. 5. Coordination environment of the potassium ion which is situated in the dimple in **1**. The potassium is coordinated to five arsenic atoms around the perimeter of the cavity and one arsenic atom in the bottom of the cavity. Selected K–As distances: K(11)–As(27) = 3.39 (1) Å, K(11)–As(2) = 3.53 (2) Å, K(11)–As(12) = 3.53 (1) Å, K(11)–As(6) = 3.57 (1) Å, K(11)–As(9) = 3.62 (2) Å, K(11)–As(8) = 3.61 (2) Å, K(16)–As(34) = 3.41 (2) Å, K(16)–As(21) = 3.45 (2) Å, K(16)–As(22) = 3.56 (2) Å, K(16)–As(17) = 3.82 (2) Å, K(16)–As(29) = 3.56 (2) Å, K(16)–As(24) = 3.90 (3) Å.

coordination to three arsenic atoms from one layer and four arsenic atoms from the opposite layer. The relatively large and equivalent isotropic displacement parameters which were observed on potassium atoms 1, 3, 5, 15, and 17 are most likely due to thermal motion, as they are not held so tightly in the lattice of atoms, rather than partial occupancy.

The structure of compound **2** also consists of layers of indium, germanium, and arsenic which are formed by $[In_5Ge_5As_{10}(As_4)]^{-5}$ polyatomic units, separated by potassium ions, as shown in Fig. 7. The original formula $K_5In_4Ge_6As_{14}$, assigned in the early stages of the structural analysis, is electron imprecise such that one electron per formula unit is forced to reside in an antibonding level (see below). Thus, the $K_5In_4Ge_6As_{14}$ formulation is unlikely to be correct, and ways of reducing one electron per formula unit (e.g., a partial deficiency in the potassium sites or a partial occupancy of In^{3+} in the Ge^{4+} sites) should be considered. The X-ray data suggests there is a partial occupancy of indium atoms in the germanium sites in $K_5In_5Ge_5As_{14}$, (**2**). The best crystallographic model which was found was a 1/6 partial occupancy of indium in each of these sites. The following numbering scheme was used: Ge(1)/In(1), Ge(2)/In(2), Ge(3)/In(3). These atoms were refined with constraints to keep each pair of atoms on one site. Originally the Ge(1), Ge(2), and Ge(3) atoms were refined as 100% germanium. This led to low equivalent isotropic displacement parameter values for Ge(1) and Ge(2), 0.99(7) and 0.84(6), respectively. The partial occupancy model led to better thermal parameters for these atoms (see Table 3), as well as a slightly better overall refinement of the structure, with $R(R_w) = 0.060(0.063)$, with GOF = 3.16 before the indium partial occupancy, and $R(R_w) = 0.056(0.057)$, with GOF = 2.87 after the indium partial occupancy. The partial occupancy model is electron precise, giving the overall formula of $K_{1.25}In_{1.25}Ge_{1.25}As_{3.5}$. The partial occupancy of indium at the germanium sites is also consistent with the lengthening of the Ge–Ge atomic distances which have an average value of 2.43 (1) Å in **1**, but are lengthened to 2.54 (4) Å in compound **2** (Table 6). This lengthening of the Ge(In)–Ge(In) bond in the $Ge_{(2-x)}In_xAs_6$ ($x \cong 1/3$) dimers is consistent with the larger atomic radius of indium versus germanium. This substitution of germanium and indium at a single site has been clearly observed previously in the compound $K_9In_9GeSb_{22}$ (11), where a partial occupancy of germanium in one of the indium sites resulted in an electron precise formulation. Assignment of the germanium and arsenic atom types in both **1** and **2** was based on the connectivity and coordination number of each atom, since germanium and arsenic cannot be distinguished simply based on X-ray diffraction data. All of the germanium atoms have tetrahedral coordination. None of the arsenic have tetrahedral coordination, which would be a geometry normally associated with As^{5+}, not As^{3-}.

When **2** is viewed down the **b** axis (Fig. 7), a view parallel to the layers, one can see a five-membered In–Ge–As ring, which is linked by a Ge(In)–Ge(In) dimer to another similar In–Ge–As five-membered ring. A six-membered ring, consisting of two Ge(In)–Ge(In) dimers, is fused to two other five-membered rings containing In, Ge, and As, through the Ge(In) dimers. This fused ring system is linked on each side to a five-membered ring through indium atoms by an arsenic atom.

In the layers of compound **2**, the $Ge_{(2-x)}In_xAs_6$ ($x \cong 1/3$) dimers and the $InAs_4$ tetrahedra are linked together, along with infinite arsenic chains, to form two-dimensional, covalently bonded sheets which run diagonally through the unit cell parallel to the (2 0 1) plane. The layers are separated by ca. 8.3 Å and are insulated from one another by interleaving regions of K^+ cations. The layers in **2** are fairly planar, compared to **1**, and lack any sort of cation-filled depressions similar to those found in compound **1**.

A polyhedral representation of a single layer of **2** is shown in Fig. 3b. The structure of the layers in **2** is best described as rows which are formed by the $Ge_{(2-x)}In_xAs_6$ ($x \cong 1/3$) dimers and the $InAs_4$ tetrahedra. As can be seen in Fig. 3b, there is a row of $Ge_{(2-x)}In_xAs_6$ ($x \cong 1/3$) dimers running through the layer, with their Ge(In)–Ge(In) bond roughly

TABLE 5
Selected Potassium Arsenic Distances (Å) for $K_8In_8Ge_5As_{17}$ (1)

Atom	Atom	Distance	Atom	Atom	Distance	Atom	Atom	Distance
K(1)	As(1)	3.185(7)	K(7)	As(19)	3.45(2)	K(12)	As(12)	3.318(8)
K(1)	As(10)	3.756(6)	K(7)	As(23)	3.40(2)	K(12)	As(14)	3.594(6)
K(1)	As(30)	3.417(6)	K(7)	As(24)	3.53(2)	K(12)	As(16)	3.513(7)
K(2)	As(1)	3.32(2)	K(7)	As(25)	3.34(2)	K(13)	As(6)	3.38(2)
K(2)	As(7)	3.30(2)	K(7)	As(33)	3.25(2)	K(13)	As(11)	3.41(2)
K(2)	As(8)	3.48(2)	K(8)	As(7)	3.32(2)	K(13)	As(12)	3.76(2)
K(2)	As(10)	3.36(2)	K(8)	As(9)	3.71(2)	K(13)	As(15)	3.83(2)
K(2)	As(30)	3.32(2)	K(8)	As(15)	3.68(2)	K(13)	As(16)	3.32(2)
K(2)	As(31)	3.80(2)	K(8)	As(23)	3.45(2)	K(13)	As(21)	3.36(2)
K(2)	As(32)	3.25(2)	K(8)	As(24)	3.44(2)	K(14)	As(5)	3.33(2)
K(3)	As(3)	3.56(2)	K(8)	As(27)	3.84(2)	K(14)	As(8)	3.46(2)
K(3)	As(13)	3.54(2)	K(8)	As(31)	3.32(2)	K(14)	As(11)	3.25(2)
K(3)	As(25)	3.36(3)	K(9)	As(1)	3.48(2)	K(14)	As(22)	3.28(2)
K(3)	As(29)	3.21(2)	K(9)	As(2)	3.57(2)	K(14)	As(28)	3.37(2)
K(4)	As(4)	3.42(2)	K(9)	As(10)	3.60(2)	K(14)	As(32)	3.35(2)
K(4)	As(7)	3.37(2)	K(9)	As(14)	3.53(2)	K(15)	As(3)	3.20(2)
K(4)	As(8)	3.59(2)	K(9)	As(15)	3.79(2)	K(15)	As(6)	3.28(2)
K(4)	As(20)	3.37(2)	K(9)	As(31)	3.30(2)	K(15)	As(9)	3.52(2)
K(4)	As(24)	3.67(2)	K(10)	As(4)	3.37(2)	K(15)	As(23)	3.19(2)
K(4)	As(32)	3.28(2)	K(10)	As(5)	3.24(2)	K(15)	As(34)	3.70(2)
K(4)	As(33)	3.43(2)	K(10)	As(17)	3.33(2)	K(16)	As(17)	3.82(2)
K(5)	As(17)	3.75(2)	K(10)	As(20)	3.22(2)	K(16)	As(21)	3.45(2)
K(5)	As(18)	3.27(2)	K(10)	As(22)	3.35(2)	K(16)	As(22)	3.56(2)
K(5)	As(19)	3.40(2)	K(10)	As(26)	3.36(2)	K(16)	As(24)	3.90(3)
K(5)	As(25)	3.40(2)	K(11)	As(2)	3.52(2)	K(16)	As(29)	3.56(2)
K(5)	As(26)	3.36(2)	K(11)	As(6)	3.57(1)	K(16)	As(34)	3.41(2)
K(6)	As(4)	3.28(2)	K(11)	As(8)	3.61(2)	K(17)	As(10)	3.52(3)
K(6)	As(18)	3.31(2)	K(11)	As(9)	3.62(2)	K(17)	As(2)	3.31(2)
K(6)	As(18)	3.45(2)	K(11)	As(12)	3.54(1)	K(17)	As(11)	3.29(2)
K(6)	As(19)	3.41(2)	K(11)	As(27)	3.39(1)	K(17)	As(14)	3.29(2)
K(6)	As(20)	3.41(2)				K(17)	As(28)	3.22(2)
K(6)	As(33)	3.42(2)				K(17)	As(30)	3.71(2)

parallel to the layer. A ball and stick view of this row of dimers can be more clearly seen in the top part of Fig. 8. The row of dimers is then connected, on either side, through corner-shared As atoms to a row of $InAs_4$ tetrahedra. This row of $InAs_4$ is connected to another row of $InAs_4$ tetrahedra, through corner-shared interactions, such that each As connecting the two rows of $InAs_4$ is a point where three $InAs_4$ tetrahedra meet. An interesting feature on the layer in **2** is an infinite chain of arsenic atoms running along either side of the $Ge_{(2-x)}In_xAs_6$ row, connecting the As atoms which are not shared between the $InAs_4$ and $Ge_{(2-x)}In_xAs_6$ polyhedra. The single crystallographically unique As–As distance along the chain is 2.529 (4) Å, which is well within the distance for an As–As bond. Finally, there is a double row of $Ge_{(2-x)}In_xAs_6$ dimers which are connected to the $InAs_4$ rows, again through corner-shared interactions. In this row, however, all the remaining As atoms are involved in the interaction between the polyhedra, and no As–As bonds are seen. The Ge(In)–Ge(In) bonds in this double row are roughly perpendicular to the layer in these rows, making the Ge(In)–Ge(In) vectors of the two different sets of $Ge_{(2-x)}In_xAs_6$ dimers approximately normal to each other. A comparison of the two types of rows of $Ge_{(2-x)}In_xAs_6$ ($x \cong 1/3$) dimers can be seen in Fig. 8.

There are three crystallographically independent potassium atoms in compound **2**, whose coordination environments are shown in Fig. 9. The potassium atom K(1) is coordinated to six arsenic atoms with K–As distances less than 3.60 Å and one longer contact of 3.71 (1) Å, with coordination to four arsenic atoms in one layer and three arsenic atoms from the adjacent layer. The atom K(2) is six-coordinate, with the arsenic atoms forming a slightly distorted octahedron. Potassium atom K(3) is coordinated by six arsenic atoms, but also has two longer interactions with As(5) and As(7) which are 3.907(9) and 3.87(1) Å, respectively. Potassium arsenic distances for **2** are given in Table 7.

The layers in both compounds **1** and **2** consist of puckered rings of indium, germanium, and arsenic which

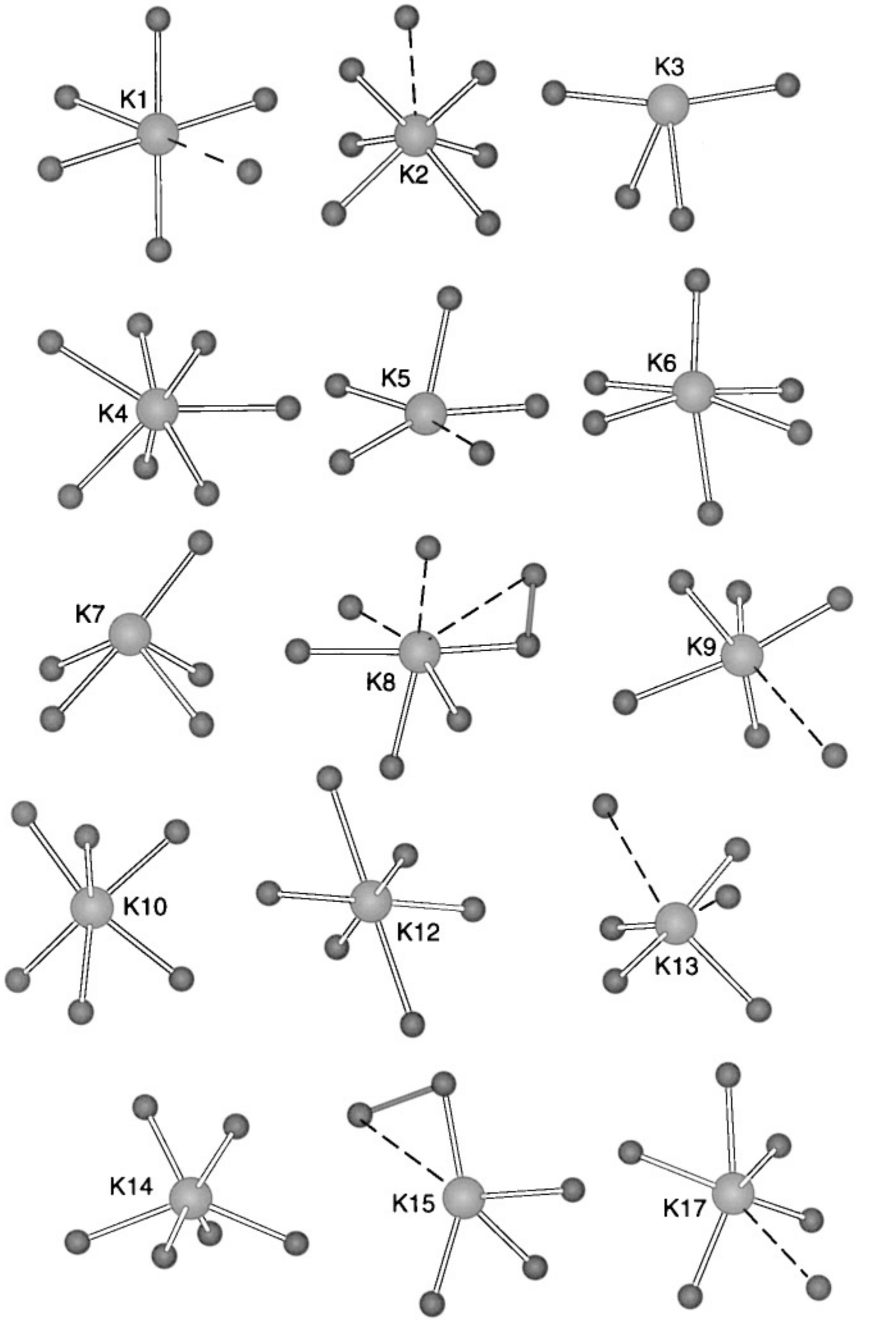

FIG. 6. Coordination environments of the potassium atoms in compound **1**. Potassium–arsenic distances are given in Table 5. Potassium-arsenic contacts up to 3.60Å are shown with solid lines and contacts between 3.60 and 3.85 Å are shown with dotted lines.

are condensed into chains within the sheets. The ring system in **2** contains components which are reminiscent of monoclinic GaTe (12), or SiAs (13), KSi_3As_3 (14), and Li_3NaSi_6 (15). The structure of GaTe and SiAs are isotypic and contain tetrahedra centered about the Ga or Si atoms formed by three Ga–Te bonds and one Ga–Ga bond, or three Si–As bonds and one Si–Si bond, respectively. These units form a six-membered ring which has two five-membered rings fused to it along the Ga–Ga or Si–Si bonds, which is further condensed to form a layered structure, as shown in Fig. 10a. The six-membered ring in GaTe is formed by two Ga_2Te_6 dimers and by two Si_2As_6 dimers in SiAs. This tricyclic unit is seen in **2** (Fig. 7) where the six-membered ring is formed by two $Ge_{(2-x)}In_xAs_6$ ($x \cong 1/3$) dimers. In the

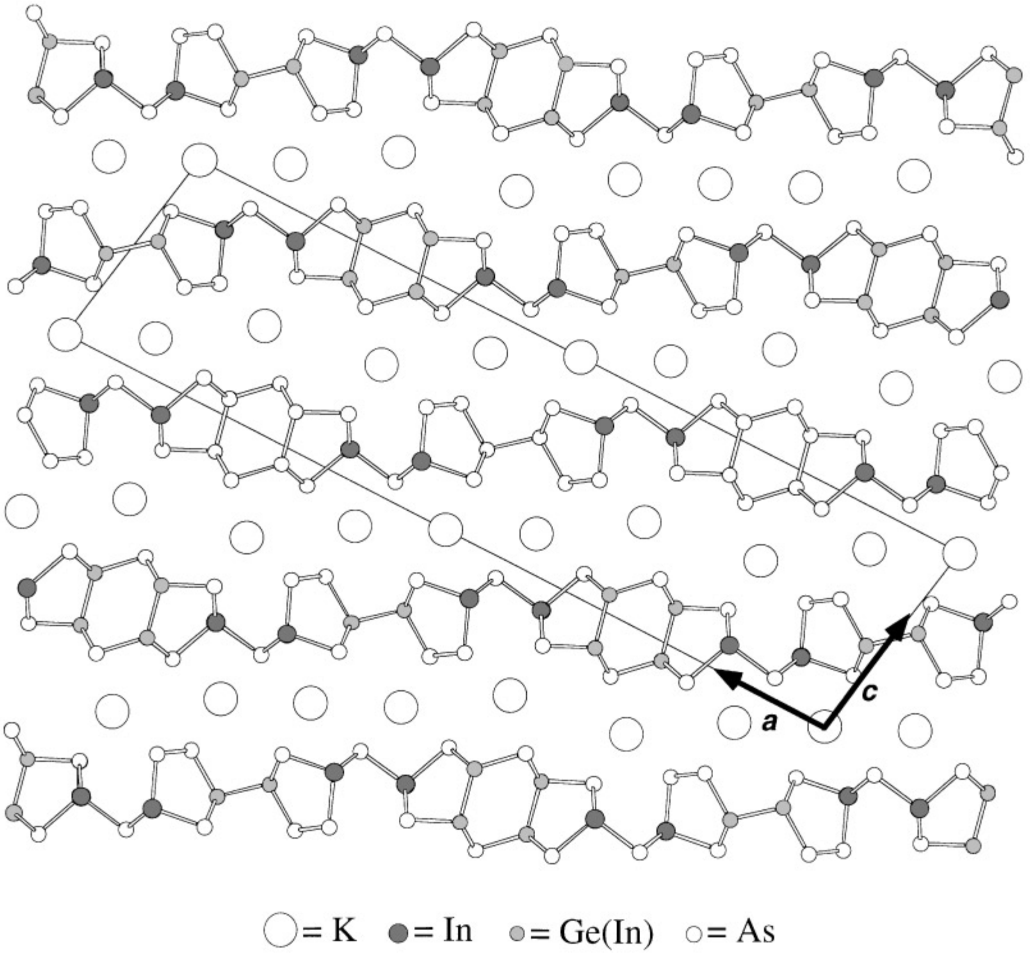

FIG. 7. View of the layered structure of $K_5In_5Ge_5As_{14}$ (**2**) down the **b** axis.

structures of GaTe and SiAs, these tricyclic units are linked through a covalent bond between the gallium or silicon atoms. In contrast to this, in compound **2**, the five-membered ring contains an indium atom and two arsenic atoms from an $InAs_4$ unit, rather than another germanium-containing unit. The tricyclic units in **2** are not directly linked to each other, but rather are separated by sets of five-membered rings.

The five-membered In–Ge–As rings in **2** are very similar to the rings which are formed in KSi_3As_3 (14). The structure of KSi_3As_3 consists of Si–As sheets which are separated by potassium cations. These sheets are formed by puckered rings of the metalloid elements which are linked together to form chains, which are further condensed to form the layers, as shown in Fig. 10b. Two five-membered rings are linked to one another through a Si–Si bond, similarly to what is seen in **2** where two of the rings are linked through a Ge(In)–Ge(In) bond. This type of linked five-membered ring system which is fused together to form layers is also seen in Li_3NaSi_6, as shown in Fig. 10c.

Both compounds **1**, $K_8In_8Ge_5As_{17}$, and **2**, $K_5In_5Ge_5As_{14}$, are electron precise materials. The oxidation state of **1** can be written as $(K^+)_8(In^{3+})_8(Ge^{3+})_5(As^{3-})_{14}(As^-)_3$, where the $+3$ charge on the Ge atom takes the Ge–Ge bond into account. Likewise, the oxidation state of **2** can be viewed as $(K^+)_5(In^{3+})_4(In^{2+})(Ge^{3+})_5(As^{3-})_{10}(As^-)_4$, where the $+3$ and $+2$ charges on the germanium and the indium atoms, respectively, take the Ge(In)–Ge(In) bond in the $Ge_{(2-x)}In_xAs_6$ ($x \cong 1/3$) dimers into account.

Electronic Structures

Bond-lengthening effect of indium partial occupation. As noted above, the "Ge–Ge" distance is 2.43 (1) Å in **1** and 2.54 (4) Å in **2**, so that the lengthening of the Ge(In)–Ge(In) bond in the $Ge_{(2-x)}In_xAs_6$ ($x \cong 1/3$) dimers is about 0.11 Å. To verify this bond lengthening effect, we optimized the staggered conformations of $H_3Ge–GeH_3$ and $H_3Ge–InH_3^-$ on the basis of DFT-MO calculations using the ADF

TABLE 6
Selected Bond Distances (Å) for $K_5In_5Ge_5As_{14}$ (2)

Atom	Atom	Distance	Atom	Atom	Distance
Ge/In(1)	Ge/In(2)	2.571(1)	In(4)	As(2)	2.658(3)
Ge/In(1)	As(1)	2.481(2)	In(4)	As(3)	2.580(2)
Ge/In(1)	As(3)	2.449(3)	In(4)	As(4)	2.604(4)
Ge/In(2)	As(1)	2.476(3)	In(5)	As(4)	2.520(3)
Ge/In(2)	As(2)	2.498(2)	In(5)	As(5)	2.555(4)
Ge/In(3)	Ge/In(3)	2.519(4)	In(5)	As(7)	2.587(4)
Ge/In(3)	As(6)	2.494(3)	As(5)	As(6)	2.529(3)
Ge/In(3)	As(7)	2.479(2)			

program (16, 17). The optimum Ge–In distance of $H_3Ge–InH_3^-$ is calculated to be larger than the optimum Ge–Ge distance of $H_3Ge–GeH_3$ by 0.30 Å (i.e., 2.690 versus 2.388 Å) (18). From the viewpoint of $K_5In_4Ge_6As_{10}(As_4)$, there are three Ge–Ge pairs per formula unit, and $K_5In_5Ge_5As_{10}(As_4)$ results when one of the three Ge–Ge bonds per formula unit is replaced with a Ge–In bond in a random fashion. Therefore, according to the geometry optimizations for $H_3Ge–GeH_3$ and $H_3Ge–InH_3^-$, the Ge(In)–Ge(In) distance of **2** is expected to be larger than the Ge–Ge distance of **1** by about 0.10 Å. This estimation is in excellent agreement with experiment.

Implications of Electron Imprecise Formulas

For a complex Zintl phase consisting of several different elements, an X-ray structure determination can give rise to several different structural formulas all with acceptable *R* factors, as found for the $K_5In_4Ge_6As_{14}$ and $K_5In_5Ge_5As_{14}$ formulations for **2**. In such a case, it is important to examine whether or not the formulas are electron precise. In terms of electronic structure, a Zintl phase has sigma bonding and sigma antibonding levels and may also possess nonbonding levels. An electron precise Zintl phase will have its bonding levels, and its nonbonding levels if present, completely filled. An electron-imprecise formula [e.g., $K_5In_4Ge_6As_{14}$] may be "electron-rich" so that the lowest-lying antibonding level is half filled (per formula unit). This

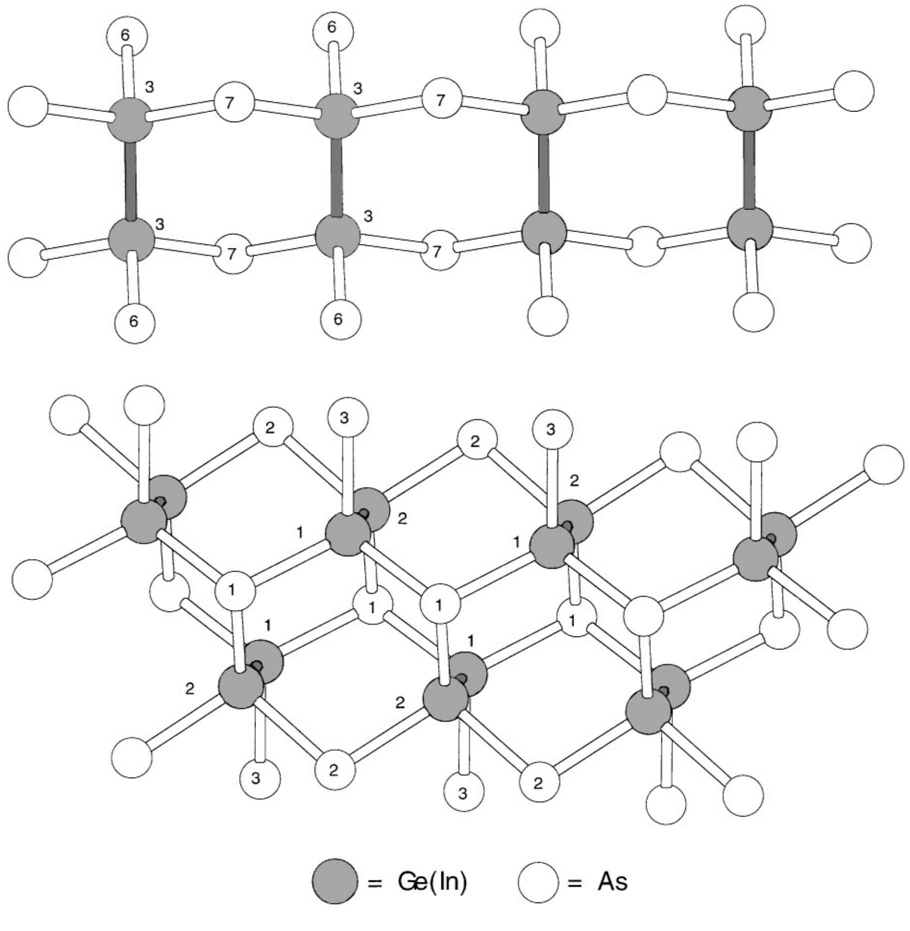

FIG. 8. Views of the two types of row formed by the $Ge_{(2-x)}In_xAs_6$ ($x \cong 1/3$) dimers in **2**.

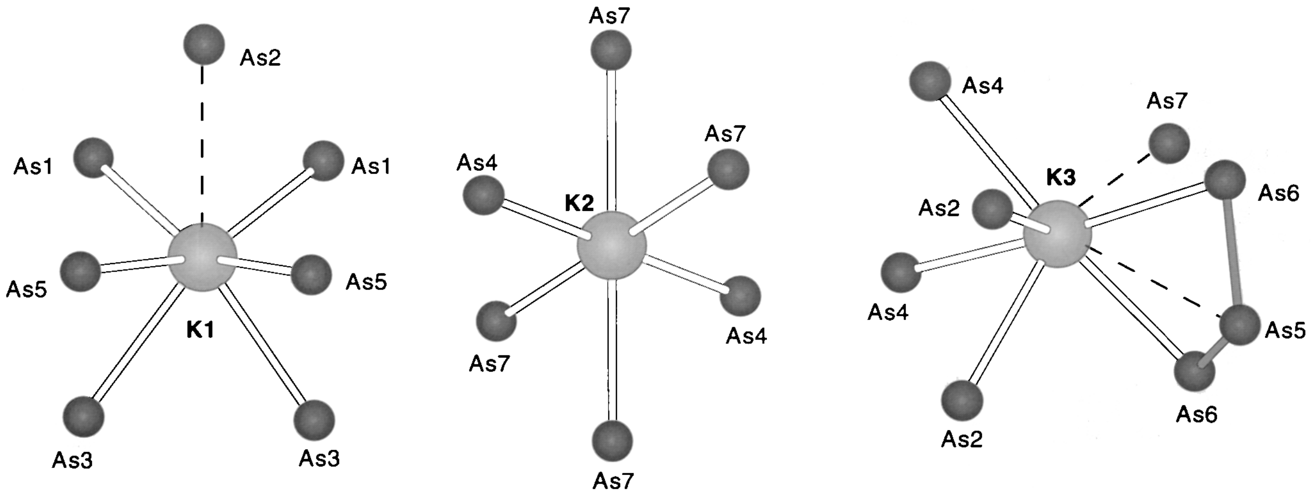

FIG. 9. Coordination environments of the potassium atoms in compound **2**. Potassium–arsenic distances are given in Table 7. Potassium–arsenic contacts up to 3.60 Å are shown with solid lines and contacts between 3.60 and 3.85 Å are shown with dotted lines.

situation is energetically unfavorable and is therefore unlikely to be correct. Such a formula should be corrected by introducing a change in chemical composition (e.g., the partial occupancy of indium atoms in the germanium sites in **2**) which will remove the electron(s) in an antibonding level thereby leading to an electron precise formula.

An electron-imprecise formula can be "electron-deficient" such that one of the highest-lying sigma bonding level is filled (per formula unit) (19). In terms of total electronic energy, this is more favorable that the "electron-rich" case when an electron occupies the lowest-lying antibonding level (per formula unit). Nevertheless, the presence of an incompletely filled sigma bonding level is unlikely to be stable. Thus, when an X-ray crystal structure determination provides an electron-imprecise formula with a half filled sigma bonding level per formula unit, it is necessary to attempt an alternative structure refinement with an electron-precise formula, which may be obtained by introducing a composition change as discussed in the previous (19) and present work. In the case when the chemical composition given by the electron-deficient formula is correct (20), one needs to consider a structural distortion (e.g., Peierls distortion) which might remove the half-filled levels (21). Namely, an alternative structure determination should be attempted with a double unit cell size. This is particularly appropriate when the structure refinement with an electron-deficient formula leads to large thermal parameters for certain atomic sites.

TABLE 7
Selected Potassium Arsenic Distances (Å) for $K_5In_5Ge_5As_{14}$ (2)

Atom	Atom	Distance	Atom	Atom	Distance
K(1)	As(1)	3.436(9)	K(3)	As(2)	3.539(9)
K(1)	As(2)	3.71(1)	K(3)	As(4)	3.412(7)
K(1)	As(3)	3.414(8)	K(3)	As(5)	3.907(9)
K(1)	As(5)	3.51(1)	K(3)	As(6)	3.375(7)
K(2)	As(4)	3.263(4)	K(3)	As(7)	3.87(1)
K(2)	As(7)	3.370(3)			

CONCLUDING REMARKS

The quaternary Zintl phases $K_8In_8Ge_5As_{17}$ (**1**) and $K_5In_5Ge_5As_{14}$ (**2**) were prepared, and their structures were determined by single crystal X-ray diffraction. Compounds **1** and **2** are representative of a new, potentially large, class of layered materials from the K–In–Ge–As system. Unlike the case of **1**, the electron-precise nature of **2** is obtained by introducing a partial occupancy of In atoms in the Ge atoms. (Indium partially occupies each of the three independent germanium sites in the ratio of 1 : 5 for In : Ge.) Without this partial occupation, the X-ray structure determination leads to an electron-imprecise formula $K_5In_4Ge_6As_{14}$ for **2**. However, this formula puts one electron per formula unit in an antibonding level and therefore is unlikely to be correct although the *R* factor of the structure determination is reasonable. Given multi-component Zintl phases with complex formulas and atoms with similar scattering factors, it is probable that X-ray structure determination can be refined for several slightly different formulas with almost equal *R* factors. From the viewpoint of bonding, the correct formulation should not have an excess electron to be accommodated in an antibonding level.

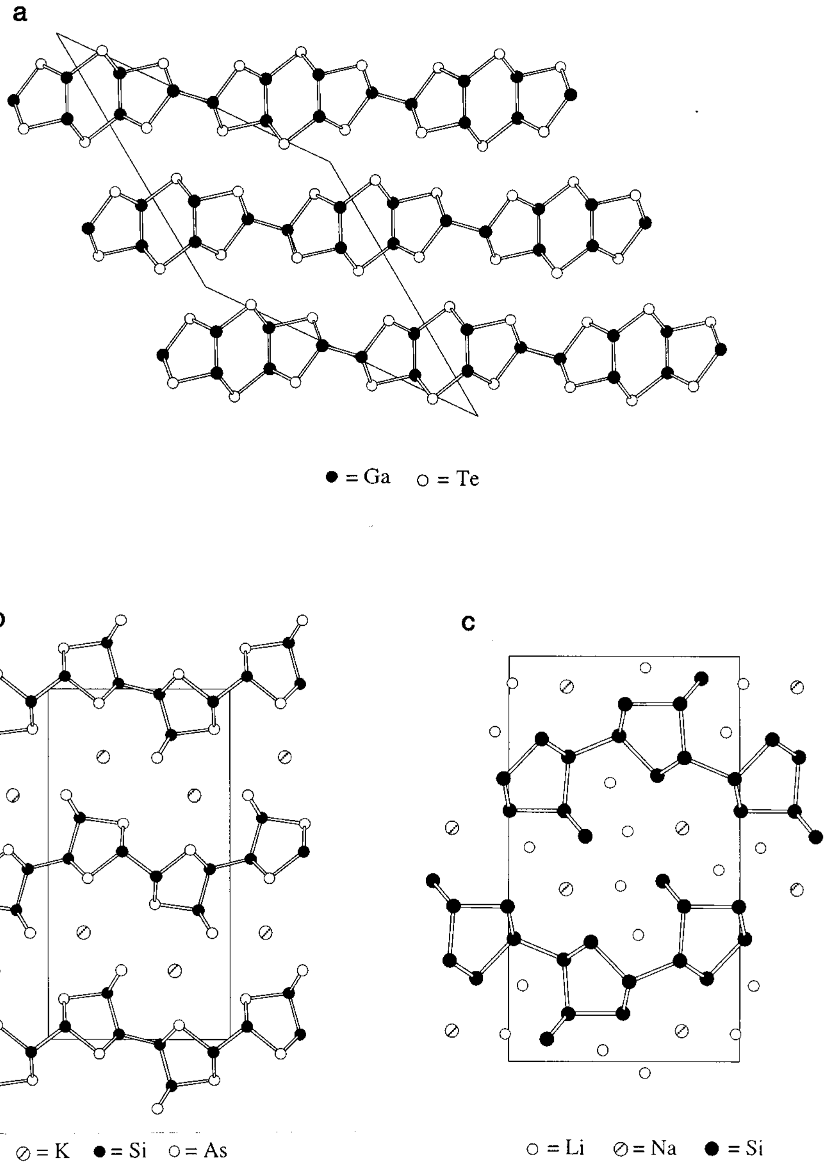

FIG. 10. (a) Structure of monoclinic GaTe. (b) Structure of KSi_3As_3. (c) Structure of Li_3NaSi_6.

ACKNOWLEDGMENT

The work at North Carolina State University was supported by the U.S. Department of Energy, Office of Basic Sciences, Division of Materials Sciences, under Grant DE-FG05-86ER45259.

REFERENCES

1. (a) I. F. Hewaidy, E. Busmann, and W. Klemm, *Z. Anorg. Allg. Chem.* **328,** 283 (1964); (b) M. Hansen, "Constitution of Binary Alloys," 2nd ed., McGraw-Hill, New York, 1958; (c) B. F. Alblas, C. van der Marel, W. Geertsma, J. A. Meijer, A. B. van Oosten, J. Dijkstra, P. C. Stein, and W. van der Lugt, *J. Non-Cryst. Solids* **61,** 201 (1984); (d) E. Busmann and S. Lohmeyer, *Z. Anorg. Allg. Chem.* **312**, 53 (1961); (e) R. Thummel and W. Klemm, *Z. Anorg. Allg. Chem.* **376**, 44 (1970); G. Bruzzone, *Acta Crystallogr. B* **25**, 1206 (1969); (f) E. Rinch and P. Feschote, *C. R. Acad. Sci.* **252**, 3592 (1961); S. Yatsenho, *Kristallografiya* **28**, 809 (1983).
2. (a) $K_2NaInSb_2$: W. Carrillo-Cabrera, N. Caroca-Canales, and H. G. von Schnering, *Z. Anorg. Allg. Chem.* **619**, 1717 (1993); (b) $K_2NaGaAs_2$, $K_2NaInAs_2$: M. Somer, K. Peters, and H. G. von Schnering, *Z. Anorg. Allg. Chem.* **613**, 19 (1992); (c) $K_2NaInAs_2$: M. Somer, K. Peters, E. M. Peters, and H. G. von Schnering, *Z. Kristallogr.* **195,** 97 (1991); (d) Cs_6InAs_3: W. Blase, G. Cordier, K. Peters, M. Somer, and H. G. von Schnering, *Angew. Chem. Int. Ed. Engl.* **30**, 326 (1991).
3. (a) $Ca_3In_2As_4$: G. Cordier, H. Schäfer, and M. Stelter, *Z. Naturforsch. B* **41**, 1416 (1986); (b) $Ca_5Sn_2As_6$: B. Eisenmann, H. Jordan, and H. Schäfer, *Z. Anorg. Allg. Chem.* **530**, 74 (1985).

4. (a) $A_3Na_{26}In_{48}$ (A = K, Rb, Cs): S. C. Sevov and J. D. Corbett, *Inorg. Chem.* **32**, 1612 (1993); (b) $Na_{15}In_{27.4}$: S. C. Sevov and J. D. Corbett, *J. Solid State Chem.* **103**, 114 (1993); (c) Rb_2In_3: S. C. Sevov and J. D. Corbett, *Z. Anorg. Allg. Chem.* **619**, 128 (1993); (d) $Na_7In_{11.8}$: S. C. Sevov and J. D. Corbett, *Inorg. Chem.* **31**, 1895 (1992); (e) K_8In_{11}: S. C. Sevov and J. D. Corbett, *Inorg. Chem.* **30**, 4875 (1991).
5. Some examples include: (a) K_6InAs_3: W. Blase, G. Cordier and M. Somer, *Z. Kristallogr.* **206**, 141 (1993); (b) $K_2In_2As_3$, $K_3In_2As_3$: G. Cordier and H. Ochmann, *Z. Kristallogr.* **197**, 293, 295 (1991); (c) Na_3InAs_2: G. Cordier and H. Ochmann, *Z. Kristallogr.* **195**, 105 (1991); (d) Cs_6InAs_3: W. Blase, G. Cordier, and M. Somer, *Z. Kristallogr.* **195**, 117 (1991); (e) $Na_{10}Ge_2As_6$: B. Eisenmann, J. Klein, and M. Somer, *Z. Kristallogr.* **197**, 265 (1991); (f) Na_4KGeAs_3: B. Eisenmann and J. Klein, *Z. Kristallogr.* **197**, 279 (1991); (g) $K_4In_4As_6$: T. L. T. Birdwhistell, C. L. Klein, T. Jefferies, E. D. Stevens, and C. J. O'Connor, *J. Mater. Chem.* **1**, 555 (1991); (h) $K_8In_6Ge_{40}$: S. Sportouch, M. Tillard-Charbonnel, and C. Belin, *Z. Kristallogr.* **209**, 541 (1994).
6. R. C. Haushalter and L. J. Krause, *Polyimides* **2**, 735 (1984); M. M. J. Treacy, R. C. Haushalter, and S. B. Rice, *Ultramicroscopy* **23**, 135 (1987); R. C. Haushalter, M. M. J. Treacy, and S. B. Rice, *Angew. Chem.* **99**, 1172 (1987); R. C. Haushalter, D. P. Goshorn, M. G. Sewchok, and C. B. Roxlo, *Mater. Res. Bull.* **22**, 761 (1987).
7. R. C. Haushalter, C. J. O'Connor, A. M. Umarji, G. K. Shenoy, and C. K. Saw, *Solid State Commun.* **49**, 929 (1984); J. W. Foise, C. J. O'Connor, and R. C. Haushalter, *Solid State Commun.* **63**, 349 (1987).
8. N. Walker and N. Stuart, N. *Acta Crystallogr. A* **39**, 158 (1983).
9. (a) DIRDIF-92: P. T. Beurskens, G. Admiraal, G. Beurskens, W. P. Bosman, S. Garcia-Granda, R. O. Gould, J. M. M. Smits, and C. Smykalla, "The DIRDIF Program System," Technical Report of the Crystallography Laboratory, University of Nijmegen, The Netherlands, 1992; (b) DIRDIF-94: P. T. Beurskins, G. Admiraal, G. Beurskins, W. P. Bosman, R. de Gelder, R. Isreal, and J. M. M. Smits, "The DIRDIF-94 Program System," Technical Report of the Crystallography Laboratory, University of Nijmegen, The Netherlands, 1994.
10. TEXSAN Single Crystal Analysis Software Package. Version 1.7-1," Molecular Structure Corporation, The Woodlands, TX, 77381, March 31, 1995.
11. J. L. Shreeve-Keyer, R. C. Haushalter, D.-K. Seo, and M.-H. Whangbo, *J. Solid State Chem.*, in press.
12. P. M. Julien-Pouzol, S. Jaulmes, M. Guittard, and F. Alapini, *Acta Crystallogr. B* **35,** 2848 (1979).
13. T. Wadsten, *Acta Chem. Scand.* **21**, 593 (1967).
14. W.-M. Hurng, J. D. Corbett, S.-L. Wang, and A. Jacobson, *Inorg. Chem.* **26**, 2392 (1987).
15. H. G. Von Schnering, M. Schwarz, and R. Nesper, *J. Less-Common Met.* **137**, 297 (1988).
16. (a) ADF Release 1.1.3, Department of Chemistry, Vrije Universiteit, Amsterdam; (b) E. J. Baerends, D. E. Ellis, and P. Ros, *Chem. Phys.* **2**, 4 (1973); (c) G. te Velde and E. J. Baerends, *J. Comp. Phys.* **99**, 84 (1992).
17. The calculations were carried out with a frozen core approximation. The valence orbitals of H were represented by double-zeta basis with polarization functions, those of Ge by triple-zeta basis with polarization functions, and those of In by triple-zeta basis without polarization functions.
18. The optimized geometrical parameters are as follows: Ge–Ge = 2.388 Å, Ge–H = 1.544 Å, and $\angle$HGeGe = 109.36° for $H_3Ge–GeH_3$. Ge–In = 2.690 Å, Ge–H = 1.580 Å, In–H = 1.827 Å, $\angle$HGeIn = 116.99° and $\angle$HInGe = 107.55° for $H_3Ge–In–H_3^-$.
19. For example, the $K_9In_{10}Sb_{22}$ formulation of the $K_9In_9GeSb_{22}$ structure. See reference (11).
20. For example, $Ba_7Ga_4Sb_9$: G. Cordier, H. Schäfer, and M. Z. Stetler, *Z. Anorg. Allg. Chem.* **543**, 137 (1986).
21. P. Alemany, S. Alvarez, and R. Hoffmann, *Inorg. Chem.* **29**, 3070 (1990).